

## Novel Templating Synthesis of Necklace-Shaped Mono- and Bimetallic Nanowires in Hybrid Organic–Inorganic Mesoporous Material

Atsushi Fukuoka,<sup>†</sup> Yuzuru Sakamoto,<sup>†</sup> Shiyu Guan,<sup>‡</sup> Shinji Inagaki,<sup>‡</sup> Noriaki Sugimoto,<sup>‡</sup> Yoshiaki Fukushima,<sup>‡</sup> Kaori Hirahara,<sup>§</sup> Sumio Iijima,<sup>§</sup> and Masaru Ichikawa\*<sup>†</sup>

Catalysis Research Center, Hokkaido University  
Sapporo 060-0811, Japan

Toyota Central R&D Laboratories, Inc.  
Nagakute, Aichi 480-1192, Japan

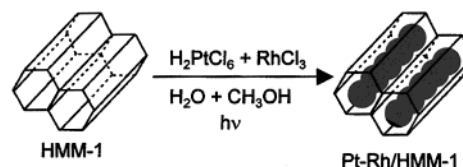
Japan Science and Technology Corporation and Department  
of Materials Science and Engineering  
Meijo University, Nagoya 468-8502, Japan

Received November 27, 2000

To control size and shape of nanocomposites has been an attractive goal in materials science and catalysis in terms of nanotechnology.<sup>1</sup> The “ship-in-bottle” synthesis is one of the promising methods for templating synthesis of metal complexes and nanocomposites in micro- and mesoporous materials.<sup>2</sup> Recently developed MCM-41,<sup>3</sup> FSM-16,<sup>4</sup> SBA-15,<sup>5</sup> organic–inorganic hybrid HMM,<sup>6</sup> and other hybrid materials<sup>7</sup> have mesopores (pore diameter 2–50 nm) to accommodate bulky metal complexes or nanocomposites, which are accessible to large substrates in catalytic reactions. HMM has a homogeneous distribution of organic (–CH<sub>2</sub>–CH<sub>2</sub>–) and inorganic (Si<sub>2</sub>O<sub>3</sub>) moieties at the molecular level in the framework, thus producing higher structural order than the inorganic silica mesoporous materials.

Nanostructured materials of transition metals are expected to show unique physical and chemical properties different from those of bulk metals. In particular, metal nanowires have attracted much attention due to their potential magnetic, optical, electrical, and catalytic properties. To date the preparation of several mono-metallic nanowires of transition metals such as Pt,<sup>8</sup> Ag,<sup>8d,9</sup> and

### Scheme 1



Au<sup>8d,10</sup> has been reported with mesoporous MCM-41, SBA-15, anodic alumina nanotubes, and carbon nanotubes as hosts. In our previous study on the preparation of Pt carbonyl clusters in NaY and FSM-16,<sup>2a,11</sup> we found that rodlike Pt nanowires were formed in FSM-16 by the photoreduction of H<sub>2</sub>PtCl<sub>6</sub>.<sup>12</sup> In this communication, we report the synthesis and characterization of novel necklace-shaped Pt–Rh, Pt–Pd, Pt, and Rh nanowires in HMM. The unique magnetic property of the Pt–Pd nanowires is also reported.

In a typical synthesis (Scheme 1), HMM-1 (2D hexagonal, pore diameter 3.1 nm, BET surface area 812 m<sup>2</sup> g<sup>−1</sup>)<sup>6a</sup> was dried under vacuum (<10<sup>−3</sup> Torr, 1 Torr = 133 Pa) at 373 K for 24 h. The dry HMM-1 was impregnated with an aqueous solution of H<sub>2</sub>PtCl<sub>6</sub>·6H<sub>2</sub>O and RhCl<sub>3</sub>·3H<sub>2</sub>O (atomic ratio Pt/Rh = 1.0, total metal loading 2.5 wt %). After drying, the sample was exposed to the vapor of water (ca. 20 Torr) for 2 h, and to that of methanol (ca. 100 Torr) for 2 h. Then the sample was irradiated with a high-pressure mercury lamp (100 W, 250–600 nm) at room temperature for 24 h. The resulting pale gray powder, designated Pt–Rh/HMM-1, was again dried under vacuum for 12 h. Pt–Pd/HMM-1 (Pt/Pd = 6.1, total metal 5 wt %) was prepared in the same method with H<sub>2</sub>PtCl<sub>6</sub>·6H<sub>2</sub>O and H<sub>2</sub>PdCl<sub>4</sub> as precursors.

A transmission electron microscope (TEM) image of Pt–Rh/HMM-1 is shown in Figure 1a, in which the nanowires are observed in the mesopores. The diameter of the wires is 3 nm in accordance with the pore size of HMM-1 (3.1 nm), and their length ranges from 10 to 50 nm (mean length 23 nm). Figure 1b is a high-resolution TEM (HRTEM) image of the Pt–Rh nanowires in HMM-1, which obviously shows that the nanowires are composed of nanoparticles connected like a necklace in the one-dimensional channel of HMM-1. The energy-dispersive X-ray (EDX) analyses were performed for the wires marked by an arrow (spot size 5 nm) in Figure 1a and for the full image of Figure 1b. The obtained Pt/Rh ratios were 1.2–1.3 for both the samples, which were similar to the ratio of charged precursors (Pt/Rh = 1.0). Furthermore, the nanowires have good crystallinity, and the wires in Figure 1b can be regarded as a single crystal because lattice fringes are observed. The observed *d* spacing is 0.23 nm, which is almost the same as the *d*(111) spacings for *fcc* Pt (0.226 nm) and Rh (0.219 nm). From the HRTEM and EDX results, we suggest that the nanowires in Pt–Rh/HMM-1 consist of the uniform Pt–Rh alloy phase.<sup>13</sup> A TEM image of Pt–Pd/HMM-1 is shown in Figure 1c, in which the length of nanowires ranges

\* To whom correspondence should be addressed. E-mail: michi@cat.hokudai.ac.jp.

<sup>†</sup> Hokkaido University.

<sup>‡</sup> Toyota Central R&D Laboratories, Inc.

<sup>§</sup> Japan Science and Technology Corporation and Meijo University.

(1) Recent reviews: (a) Bradley, J. S. In *Clusters and Colloids*; Schmid, G., Ed.; VCH: Weinheim, 1994; pp 459–544. (b) Schmid, G. In *Applied Organometallic Catalysis with Organometallic Compounds*; Cornils, B., Herrmann, W. A., Eds.; VCH: Weinheim, 1996; pp 636–644.

(2) (a) Ichikawa, M. In *Metal Clusters and Catalysis*; Braunstein, P., Oro, L. A., Raithby, P. R., Eds.; Wiley-VCH: Weinheim, 1999; pp 1273–1301. (b) Kawi, S.; Gates, B. C. In *Clusters and Colloids*; Schmid, G., Ed.; VCH: Weinheim, 1994; pp 299–372. (c) Schulz-Ekloff, G.; Ernst, S. In *Handbook of Heterogeneous Catalysis*; Ertl, G., Knözinger, H., Weitkamp, J., Eds.; Wiley-VCH: Weinheim, 1997; pp 374–387. (d) Ichikawa, M. *Platinum Metals Rev.* **2000**, *44*, 3–14.

(3) (a) Kresge, C. T.; Leonowicz, M. E.; Roth, W. J.; Vartuli, J. C.; Beck, J. S. *Nature* **1992**, *359*, 710–712. (b) Beck, J. S.; Vartuli, J. C.; Roth, W. J.; Leonowicz, M. E.; Kresge, C. T.; Schmitt, K. D.; Chu, C. T.-W.; Olson, D. H.; Sheppard, E. W.; McCullen, S. B.; Higgins, J. B.; Schlenker, J. L. *J. Am. Chem. Soc.* **1992**, *114*, 10834–10843.

(4) (a) Inagaki, S.; Fukushima, Y.; Kuroda, K. *J. Chem. Soc., Chem. Commun.* **1993**, 680–682. (b) Inagaki, S.; Koiwai, A.; Suzuki, N.; Fukushima, Y.; Kuroda, K. *Bull. Chem. Soc. Jpn.* **1996**, *69*, 1449–1457.

(5) Zhao, D.; Feng, J.; Huo, Q.; Melosh, N.; Fredrickson, G. H.; Chmelka, B. F.; Stucky, G. D. *Science* **1998**, *279*, 548–552.

(6) (a) Inagaki, S.; Guan, S.; Fukushima, Y.; Ohsuna, T.; Terasaki, O. *J. Am. Chem. Soc.* **1999**, *121*, 9611–9614. (b) Guan, S.; Inagaki, S.; Ohsuna, T.; Terasaki, O. *J. Am. Chem. Soc.* **2000**, *122*, 5660–5661.

(7) (a) Asefa, T.; MacLachian, M. J.; Coombs, N.; Ozin, G. A. *Nature* **1999**, *402*, 867–871. (b) Yoshina-Ishii, C.; Asefa, T.; Coombs, N.; MacLachian, M. J.; Ozin, G. A. *Chem. Commun.* **1999**, 2539–2540. (c) Corriu, R. J. P.; Hoarau, C.; Mehdi, A.; Reyé, C. *Chem. Commun.* **2000**, 71–72.

(8) (a) Ko, C. H.; Ryoo, R. *Chem. Commun.* **1996**, 2467–2468. (b) Liu, Z.; Sakamoto, Y.; Ohsuna, T.; Hiraga, T.; Terasaki, O.; Ko, C. H.; Shin, H. J.; Ryoo, R. *Angew. Chem., Int. Ed.* **2000**, *39*, 3107–3110. (c) Kyotani, T.; Tsai, L.; Tomita, A. *Chem. Commun.* **1997**, 701–702. (d) Han, Y.; Kim, J. M.; Stucky, G. D. *Chem. Mater.* **2000**, *12*, 2068–2069.

(9) (a) Huang, M. H.; Choudrey, A.; Yang, P. *Chem. Commun.* **2000**, 1063–1064. (b) Plyuto, J.; Berquier, J.; Jacquod, C.; Ricolleau, C. *Chem. Commun.* **1999**, 1653–1654.

(10) Hornyak, G.; Kröll, M.; Pugin, R.; Sawitowski, T.; Schmid, G.; Bovin, J.; Karsson, G.; Hofmeister, H.; Hopfe, S. *Chem. Eur. J.* **1997**, *3*, 1951–1956.

(11) (a) Rao, L.; Fukuoka, A.; Ichikawa, M. *J. Chem. Commun., Chem. Commun.* **1988**, 458–460. (b) Rao, L.; Fukuoka, A.; Kosugi, N.; Kuroda, H.; Ichikawa, M. *J. Phys. Chem.* **1990**, *94*, 5317–5327. (c) Yamamoto, T.; Shido, T.; Inagaki, S.; Fukushima, Y.; Ichikawa, M. *J. Am. Chem. Soc.* **1996**, *118*, 5810–5811. (d) Yamamoto, T.; Shido, T.; Inagaki, S.; Fukushima, Y.; Ichikawa, M. *J. Phys. Chem. B* **1998**, *102*, 3866–3875. (e) Fukuoka, A.; Osada, M.; Shido, T.; Inagaki, S.; Fukushima, Y.; Ichikawa, M. *Inorg. Chim. Acta* **1999**, *294*, 281–284.

(12) (a) Sasaki, M.; Osada, M.; Sugimoto, N.; Inagaki, S.; Fukushima, Y.; Fukuoka, A.; Ichikawa, M. *Microporous Mesoporous Mater.* **1998**, *21*, 597–606. (b) Sasaki, M.; Osada, M.; Higashimoto, N.; Yamamoto, T.; Fukuoka, A.; Ichikawa, M. *J. Mol. Catal. A* **1999**, *141*, 223–240.

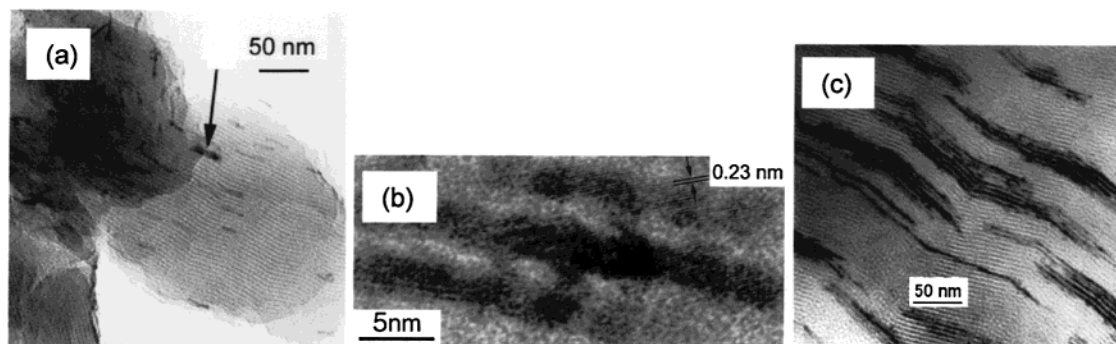


**Figure 1.** (a) A TEM (JEOL JEM-2000ES, 200 kV) image of Pt–Rh nanowires in HMM-1. (b) An HRTEM (JEOL JEM-2010F, 100 kV) image of Pt–Rh nanowires in HMM-1. (c) A TEM (Hitachi H-800, 200 kV) image of Pt–Pd nanowires in HMM-1.

from 10 to 350 nm (mean length 170 nm). The EDX analysis suggests that the nanowires are bimetallic; the observed Pt/Pd ratios are 6.4–7.3 and the charged one is 6.1.

Monometallic Pt or Rh nanowires were also prepared by the photoreduction of  $\text{H}_2\text{PtCl}_6 \cdot 6\text{H}_2\text{O}$  or  $\text{RhCl}_3 \cdot 3\text{H}_2\text{O}$  in HMM-1. The Pt nanowires in HMM-1 (Pt 5 wt %) have the diameter of 3 nm, and the length is 10–250 nm (mean length 120 nm). In the Pt L<sub>II</sub>- and L<sub>III</sub>-edge X-ray absorption near-edge structure (XANES) studies measured at 20 K, the number of unfilled *d* state per Pt atom for Pt/HMM-1 is estimated to be 0.351 by assuming that the number for Pt foil is 0.300.<sup>15</sup> Therefore, the oxidation state of the Pt nanowires in HMM-1 is Pt(0), but they are slightly electron-deficient compared to bulk Pt. The Rh nanowires in HMM-1 (Rh 2.5 wt %) have the length of 10–140 nm (mean length 48 nm). The Pt and Rh nanowires also show the necklace-like structure in the TEM images.

The powder X-ray diffraction (XRD) patterns for the Pt, Rh, Pt–Rh, and Pt–Pd/HMM-1 exhibited peaks of (100), (110), and (200) at 1–4° due to a 2D hexagonal structure of HMM-1. No significant change of the low-angle peaks was observed after the photoreduction procedure, indicating that the pore structure of HMM-1 was maintained in the formation of nanowires. Typical peaks of metal crystallites appeared at 35–85° for the four samples after the photoreduction.

The necklace-shaped morphology consisting of the connected nanoparticles is characteristic of the nanowires formed in HMM-1. The maximum diameter of the nanonecklace is 3.1 nm, the minimum one at the nodes is 1.8–2.0 nm, and the length of the particles is 3–5 nm. In contrast, rodlike nanowires with smooth surfaces are formed in FSM-16, MCM-41, and SBA-15,<sup>8,9,12</sup> thus implying that the necklace-structure is ascribed to the interaction with the internal surface of HMM-1 having organic spacers in the silica fragments. This structure of Pt nanowires in HMM-1 remained unchanged with heating at 473 K under vacuum.

(13) Preliminary extended X-ray absorption fine structure (EXAFS) studies indicate the formation of the Pt–Rh bonding for Pt–Rh/HMM-1. However, further study is needed for the compositional homogeneity of Pt and Rh.<sup>14</sup> Detailed EXAFS characterization is now in progress.

(14) (a) Harada, M.; Asakura, K.; Toshima, N. *J. Phys. Chem.* **1994**, *98*, 2653–2662. (b) Cimini, F.; Prins, R. *J. Phys. Chem. B* **1997**, *101*, 5285–5293.

(15) Mansour, A. N.; Cook, J. W., Jr.; Sayers, D. E.; Emrich, R. J.; Katzer, J. R. *J. Catal.* **1984**, *89*, 462–469.

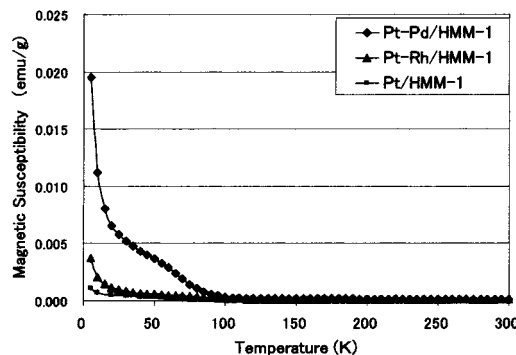


**Figure 2.** Temperature dependence of magnetic susceptibility for Pt–Pd/HMM-1 (Pt/Pd = 6.1, total metal 5 wt %), Pt–Rh/HMM-1 (Pt/Rh = 1.0, total metal 2.5 wt %), and Pt/HMM-1 (Pt 5 wt %).

Figure 2 exhibits the temperature dependence of the magnetization data for the Pt–Pd, Pt–Rh, and Pt wires in HMM-1. The magnetic susceptibilities of the three samples seem to obey Curie's law, although some deviation from the law is observed for Pt–Pd/HMM-1 at around 60 K. Interestingly, the Pt–Pd system shows a great increase in the magnetic susceptibility as cooling below 90 K, while the Pt–Rh and Pt systems give lower magnetization. The magnetization for Pt–Pd/HMM-1 is two or three times higher than expected from the simple sum of the values of bulk Pt and Pd.<sup>16</sup> The unusual enhancement of the magnetization for Pt–Pd/HMM-1 may be attributable to the low-dimensionality of the metal topology.

**Acknowledgment.** This work was supported by a Grant-in-Aid for Scientific Research from the Ministry of Education, Science, Sports and Culture, Japan (No. 11650803).

**Supporting Information Available:** TEM images of Pt/HMM-1 and Rh/HMM-1, and XRD profiles of Pt, Rh, Pt–Rh, and Pt–Pd/HMM-1 (PDF). This material is available free of charge via the Internet at <http://pubs.acs.org>.

JA004067Y

(16) (a) García, A. E.; González-Robles, V.; Baquero, R. *Phys. Rev. B* **1999**, *59*, 9392–9401. (b) Lee, K. *Phys. Rev. B* **1998**, *58*, 2391–2394. (c) Cox, A. J.; Louderback, J. G.; Apsel, S. E.; Bloomfield, L. A. *Phys. Rev. B* **1994**, *49*, 12295–12298.